Silicon Nanocrystals: Size Matters**

By *Johannes Heitmann*, *Frank Müller*, *Margit Zacharias*,* and *Ulrich Gösele*

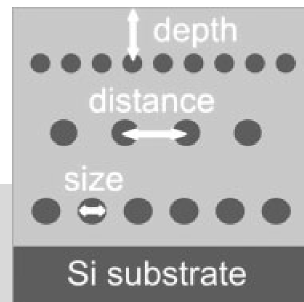

This paper reviews new approaches to size-controlled silicon-nanocrystal synthesis. These approaches allow narrowing of the size distribution of the nanocrystals compared with those obtained by conventional synthesis processes such as ion implantation into SiO_2 or phase separation of sub-stoichiometric SiO_x layers. This size control is realized by different approaches to introducing a superlattice-like structure into the synthesis process, by velocity selection of silicon aerosols, or by the use of electron lithography and subsequent oxidation processes. Nanocrystals between 2 and 20 nm in size with a full width at half maximum of the size distribution of 1 nm can be synthesized and area densities above 10^{12} cm^{-2} can be achieved. The role of surface passivation is elucidated by comparing Si/SiO_2 layers with superlattices of fully passivated silicon nanocrystals within a SiO_2 matrix. The demands on silicon nanocrystals for various applications such as non-volatile memories or light-emitting devices are discussed for different size-controlled nanocrystal synthesis approaches.

1. Introduction

The first experimental results more than a decade ago demonstrating room-temperature luminescence of silicon nanocrystals (Si-NCs) in silicon-implanted SiO_2[1] or in porous silicon[2,3] triggered a strong interest in the fabrication of Si-NCs and their properties. Besides fundamental physics questions concerning quantum-confinement effects in the indirect semiconductor silicon,[4–7] potential applications such as light emission from electrically excited Si-NCs,[8–13] energy transfer to Er^{3+} ions,[14–19] and non-volatile memory devices[20,21] also stimulated a broad interest in this material system. For clarifying the origin of the observed luminescence signal as well as for the described potential applications, tight control over the size of the nanocrystals is essential. Synthesis of Si-NCs can be realized by electrochemically etching single-crystalline silicon in hydrofluoric acid, resulting in a sponge-like structure called porous silicon;[3,6,22] by ion implantation of silicon into an SiO_2 matrix followed by thermally induced Ostwald ripening of silicon clusters and their crystallization;[23–26] by deposition of sub-stoichiometric oxide films using chemical vapor deposition (CVD);[27–30] by sputtering processes;[31–36] or by reactive evaporation[37] followed by a thermally induced phase separation and crystallization of the Si-NCs. All these methods result in a relatively broad size distribution of the synthesized Si-NCs. Size control in these systems is normally realized by shrinking the entire size distribution by varying the silicon content within the SiO_2 matrix,[38] by changing the etching conditions in the case of porous silicon,[39] or by subsequent oxidation of the nanocrystals.[40] The resulting broad size distributions complicate the characterization of quantum-confinement effects and are undesirable for potential applications of these structures. In the case of optical characterization, this problem can be partially circumvented by resonant excitation, which results in a narrowing of the excited size distribution.[4–6] These experiments could only be successfully realized for porous silicon due to the availability of thick films (i.e., large numbers of nanocrystals) which can be synthesized by this method. Especially in the case of thin SiO_2 layers containing Si-NCs, the density of Si-NCs of one size is too small for this kind of investigation.

In recent years, new ways of narrowing the size distribution of the Si-NCs have been developed by introducing new tech-

[*] Prof. M. Zacharias, J. Heitmann,[+] Dr. F. Müller, Prof. U. Gösele
Max-Planck-Institut für Mikrostrukturphysik
Weinberg 2, D-06120 Halle (Germany)
E-mail: zacharias@mpi-halle.de

[+] Present address: Infineon Technologies Dresden, PF 100940, D-01076 Dresden, Germany.

[**] We thank L. X. Yi, R. Scholz, and H. Hofmeister for fruitful collaboration in the area of SiO_x/SiO_2 superlattices and the German Science Foundation (DFG) for supporting part of the work described in this paper.

 DOI: 10.1002/adma.200401126 © 2005 WILEY-VCH Verlag GmbH & Co. KGaA, Weinheim

niques to the synthesis process. This paper reviews the most prominent and promising recently developed approaches for the synthesis of narrow size distributions of Si-NCs and discusses their potential for applications.

2. Applications and New Perspectives

In this section, we discuss the need for size control in the Si-NC system to investigate basic quantum-confinement effects and for potential applications. From the various potential applications suggested for Si-NCs, we have chosen electrically pumped light emission and non-volatile memories.

2.1. Optical Characterization

The origin of the room-temperature photoluminescence (PL) signal from Si-NCs is still under discussion, and some essential features of this PL signal are still not understood in detail. Several mechanisms have been suggested to explain the appearance of this luminescence signal, such as defects within the SiO_2[41,42] or at the nanocrystal surface,[43–46] the formation of siloxene,[47–49] or quantum-confinement effects of the excitons caused by their spatial confinement within the Si-NCs.[3,4,6] For porous silicon, the latter mechanism was proved to be the origin of the observed luminescence by the appearance of silicon phonon-related structures in the resonantly excited PL signal.[4,6] For Si-NC within an oxide matrix, this discussion is still ongoing and the answer might be different for different sample systems. Even if one assumes that quantum confinement is the origin of this luminescence band, this effect can not easily be separated from other effects such as the migration of excitons[50–53] due to the broad size distribution of the Si-NCs involved.

Hence, for optical characterization tight control of the crystal size and a corresponding narrow size distribution are essential. Optical measurements performed on individual silicon quantum dots show very interesting results,[54,55] but for a better understanding of various features, such as the full width at half maximum (FWHM) value of more than 100 meV for the PL signal, low-temperature measurements are required. Such measurements are only possible for a sufficiently large quantity of monodisperse nanocrystals because of the low recombination probabilities at low temperatures. These monodisperse nanocrystals have to be well passivated by SiO_2 in order to obtain a measurable luminescence signal and to ensure that the observed luminescence is caused by quantum-confinement effects.

2.2. Electrically Pumped Light Emission from Silicon

Even after more than ten years of research on room-temperature photoluminescent porous silicon, a commercial silicon-based light-emitting diode (LED) based on quantum-confined luminescence in the near infrared is still not available. Electroluminescence (EL) measurements on all sorts of Si-NCs show efficiencies below 1×10^{-3}.[8–13] This makes electrically pumped light emission from Si-NCs unattractive for industrial applications at the moment. Size control and ordered arrangements of the nanocrystals will make light emission more efficient and could decrease the required voltages. Nevertheless, even an increase of a factor of ten in efficiency would not drastically change the situation with regard to potential applications. The bandgap remains indirect, even for very small crystallites, and the quantum efficiency of a Si-NC is limited to one photon per lifetime due to very efficient Auger recombination processes within the nanocrystal.[5] The lifetime of the quantum-confined silicon luminescence is about 10 to 100 µs depending on crystal size and measuring temperatures.

The situation changes if one uses the Si-NCs as sensitizers for other active elements, such as Er^{3+} ions. The Er^{3+} luminescence at 1.54 µm is of great technological interest due to the absorption minimum of SiO_2-glass fibers in this wavelength range. The very small absorption cross-section of erbium prevents effective application of Er^{3+} in integrated optoelectronics, and so the use of appropriate sensitizers such as Si-NCs, which can transfer their energy to the Er^{3+} ions, is highly desirable. The very effective energy transfer to Er^{3+} ions also allows the fabrication of efficient electrically pumped devices. Recently, ST Microelectronics reported an Er/Si-NC LED with 10 % efficiency, which is the current record for silicon-

Margit Zacharias received her habilitation in experimental physics at the University of Magdeburg in 1999. Prior to that, she had a visiting professorship at the Department of Electrical and Computer Engineering at the University of Rochester, Rochester, NY, in 1996. Since 2000, she has been the head of the Nanowires & Nanoparticle group at the Experimental Department II of the Max Planck Institute of Microstructure Physics, Halle, Germany. Her research interests include photonic crystals, quantum effects in silicon and germanium nanocrystals, and self-organized nanostructure formation, including nanowire growth and properties. Since June 2004, she has coordinated the priority program on nanowires and nanotubes of the German Research Foundation (SPP 1165).

© 2005 WILEY-VCH Verlag GmbH & Co. KGaA, Weinheim

based light emission.[56] This device does not utilize any additional control of the crystal size besides the conventional phase separation of bulk SiO_x layers. A device with a narrow Si-NC size distribution should show an even higher efficiency. This narrow size distribution would also facilitate adjusting the Si-NC (sensitizer) emission wavelength to the absorption levels of Er^{3+} as discussed below.

2.3. Non-Volatile Memories Based on Si-NCs

Si-NCs in oxide matrixes are serious candidates for the next generation of non-volatile memories.[20,21] The working principle is shown in Figure 1.[20] A thin (1–2 nm) tunneling oxide separates the inversion surface of an n-channel silicon field-effect transistor (FET) from a distributed film of Si-NCs that covers the entire surface-channel region. A thicker tunneling

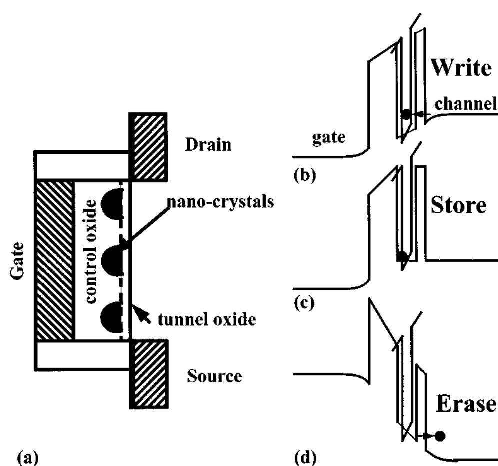

Figure 1. a) Schematic cross-section of a Si-NC based non-volatile memory and its band diagram for b) writing, c) storing, and d) erasing. (Reprinted with permission from [20]. Copyright 1996 American Institute of Physics.)

oxide separates the nanocrystals from the control gate of the FET. Electron injection occurs from the inversion layer via direct tunneling when the control gate is forward biased with respect to the source and drain. For gate oxides with thicknesses between 2 and 5 nm, the retention times for these non-volatile memories should be comparable to commercially available EEPROMs (electrically erasable programmable read-only memories). However, results demonstrating longer retention times for Si-NCs have not yet been shown. The working principle outlined in Figure 1 implies that the best configuration for this approach would be a single layer of monodisperse Si-NCs. A key requirement for this application is the independent control of the Si-NC size and the inter-nanocrystal distance in order to reach the highest possible area density of Si-NCs without any tunneling between neighboring nanocrystals of the stored electrons.

3. Size-Controlled Silicon-Nanocrystal Synthesis

3.1. Amorphous Silicon/Insulator Superlattices

The use of Si/SiO_2 superlattices was first introduced by Lockwood and co-workers.[57,58] In this technique, molecular-beam epitaxy (MBE) combined with oxidization by UV/ozone is used to precisely grow nanometer-thick amorphous silicon layers in between SiO_2 layers. Quantum-confinement effects of the amorphous silicon layers were investigated.[57] The observed room-temperature PL peak position depends on the silicon-layer thickness and was fitted by the effective-mass approximation. Later, similar systems could be realized by reactive magnetron sputtering or co-sputtering,[59–63] plasma-enhanced (PE)CVD or low-pressure (LP)CVD,[64–66] or reactive evaporation.[67] After the crystallization of the amorphous silicon layers, the passivation of the often brick-shaped Si-NC surface plays a major role. Often the luminescence signal is reduced by non-radiative processes or dominated by radiative recombination processes at special defects, which may be formed at the nanocluster interface or cannot (at least, not clearly) be assigned to a quantum-confined origin.[58,60,63] Additional treatment of the samples with H_2 or O_2 improves the passivation of the Si-NC surface so that in a few cases the appearing luminescence signal could clearly be assigned to a quantum-confined origin.[68] The Si-NCs show a brick-like shape,[62,68] and their size can be controlled by the initial thickness of the amorphous Si layers as shown in Figure 2. Grain boundaries exist between the different brick-like Si-NCs, which are undesirable because of their potential to contain numerous non-radiative recombination centers. The presence of grain boundaries is a kind of "birth defect" of the amor-

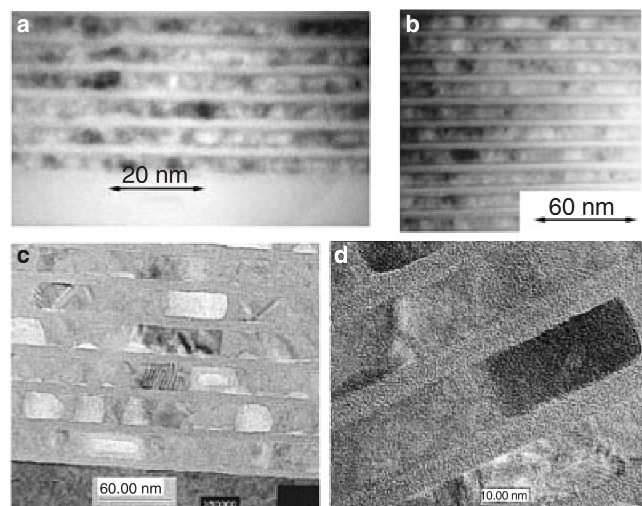

Figure 2. Crystallized amorphous Si/SiO_2 superlattices with a) 4.2 nm, b) 8.5 nm, and c) 20 nm Si layer thicknesses. d) The magnified image of a brick-shaped Si-NC with 20 nm vertical and 50 nm lateral dimensions. (Reprinted with permission from [68]. Copyright 2000 Nature Publishing Group.)

 © 2005 WILEY-VCH Verlag GmbH & Co. KGaA, Weinheim

phous silicon layer approach. An approach to avoid these defects will be discussed in Section 3.2. The crystallization process in the layered arrangement of the amorphous silicon within the insulating matrix leads to a drastic change of the critical crystallization energy.[69] The crystallization temperature increases for decreasing crystal size compared to values for bulk silicon.[62,70] A combination of this controlled deposition method with a patterning of the resulting layered structure comparable to other microelectronic devices is possible.[71,72] Especially in the work of Striemer et al.,[72] the pre-patterning of the substrate provided additional control of the crystallization position of individual crystals.

The approach of using ultrathin amorphous Si layers between insulating materials can also be adapted to a number of different materials. The growth of Si-NC:H/a-Si:H was realized by radiofrequency-sputtering methods as shown by Wu et al.[73] Si/SiN_x superlattices were synthesized by electron-gun silicon evaporation and periodic electron cyclotron resonance plasma nitridation,[74] by excimer pulsed-laser deposition,[12,75] and by LPCVD.[76,77] $Si/Si_xO_yN_z$ superlattices were produced by LPCVD.[78] Finally, Si/CaF_2 superlattices were synthesized by room-temperature MBE.[79,80]

These controlled deposition methods led to a number of diode-like structures for electrically pumped devices.[12,81–83] Also, for the EL measurements, different signal wavelengths between 500 and 900 nm were reported; these were mainly attributed to hot-impact ionization of excitons confined in the Si-NCs. This explanation could not be proved in detail and is still under discussion. The reported quantum efficiencies of electroluminescence do not exceed 1×10^{-3}.

The potential of these structures for non-volatile memory applications could be shown by the appearance of a hysteresis loop in the conductance–voltage (C–V) measurements of such structures.[59,61] This was made possible by controlled recrystallization and passivation by short-time steam oxidation of the nanocrystal interfaces.[59]

Erbium doping of the crystallized Si/SiO_2 superlattices was carried out[84,85] in order to use Si-NCs as sensitizers for Er^{3+} luminescence. The reported transfer efficiencies increase with decreasing silicon-layer thickness,[84] but are quite low compared to isolated Si-NCs synthesized conventionally by cosputtering of sub-stoichiometric oxides or ion implantation.[14–19] Energy transfer from amorphous Si/SiO_2 superlattices was also reported.[86] In this case, an exponential distance dependence was reported, which so far has not been possible to measure for crystallized samples.

The main problem of Si-NC synthesis via superlattices involving amorphous silicon is the required passivation of the nanocrystal surfaces and, especially, the nanocrystal/nanocrystal grain boundaries, as mentioned above. At the grain boundaries between the Si-NCs defects like silicon dangling bonds can occur, and can either dominate the PL signal or create non-radiative recombination centers for electron–hole pairs at the nanocluster/nanocluster interface. This is the reason for the large number of different PL bands observed in samples based on amorphous Si/SiO_2 and the rather low PL intensities in comparison with conventionally fabricated samples. For applications in the area of nonvolatile memories, a passivated surface of the nanocrystals is also essential. Subsequent oxidization steps after the superlattice growth were introduced to overcome this problem.

3.2. Superlattices and Single Layers of Passivated Si-NCs in SiO_2

As mentioned above, the main problem of the Si-NC synthesis via the crystallization of amorphous silicon/insulator superlattices is the passivation of the nanocluster/nanocluster interfaces. One way to synthesize passivated nanocrystals would be to introduce the required passivation step directly into the deposition procedure. This was realized by the LPCVD-assisted silicon-dot formation method where an additional oxidation step was introduced directly after the formation of the silicon dots.[87] This procedure was then repeated up to six times, resulting in the formation of a superlattice of well-passivated Si-NCs. The observed PL signal shows a size-dependent blue-shift which most likely originates from quantum-confinement effects, even though the authors[87] prefer to use surface states to explain the blue-shift.

The formation of just one layer of Si-NCs by LPCVD on different substrate layers such as SiO_2, Si_3N_4, and SiO_xN_y was demonstrated by LPCVD of SiH_4 followed by oxidation.[88] For nanocrystals on the SiO_2 surface, current–voltage (I–V) characteristics of single nanocrystals were measured and showed a Coulomb gap of 0.19–0.25 V with staircases between 0.06 and 0.07 V. The size distribution over the whole sample is still rather broad (FWHM: 3–4 nm),[88] but due to the spatial resolution of atomic force microscopy (AFM), the measurements allow examination of single nanocrystals, thus providing an accurate determination of the size dependence of the measured effects.[89] This growth of one layer of isolated Si-NCs by LPCVD could also be shown by a number of other authors.[90–92] Area densities up to 10^{12} cm^{-2} were achieved by this synthesis method.[90] Excellent performance in terms of charge storage and retention times was shown.[90,91] In the work of Ioannou-Sougleridis et al.,[92] this deposition method was used to investigate the quantum-confined Stark effect by PL spectroscopy under external electric fields.

A method for forming a monolayer of well-defined Si-NCs passivated by SiO_2 by ion implantation was theoretically proposed by Müller et al.[93] In this proposal, low-energy silicon-ion implantation (1 keV) into thin oxide layers would lead to the formation of a single Si-NC layer. For specific implantation and annealing conditions, the formation of a single layer of Si-NCs 2–3 nm in size and with area densities higher than 10^{12} crystals per square centimeter was predicted. Above a certain implantation dose ($\sim 10^{16}$ cm^{-2}), percolation would lead to a spatially connected two-dimensional silicon pattern. For an implantation dose of 10^{16} cm^{-2}, experimental results show charge-trapping behavior, as would be expected from excess silicon in SiO_2; for higher doses (2×10^{16} cm^{-2}), a peri-

© 2005 WILEY-VCH Verlag GmbH & Co. KGaA, Weinheim

odic staircase plateau in the *I–V* characterization supports the suggestion that single nanocrystals act as charge-trapping centers.[94]

A relatively new approach for tight control of the size distribution of Si-NCs uses the phase separation of ultrathin SiO_x layers within SiO_x/SiO_2 superlattices,[95] where $1 \leq x < 2$. This phase separation is a well-defined process in which the annealing of the SiO_x/SiO_2 superlattices results in the formation of amorphous silicon clusters in an SiO_2 matrix at lower annealing temperatures, which then crystallize at annealing temperatures above 900 °C.[96] In Figure 3 the resulting superlattices of size-controlled Si-NCs (FWHM < 1 nm) with surfaces well-passivated by SiO_2 are shown. The size of the nanocrystals is controlled by the SiO_x layer thickness. The blue-shift of the photoluminescence as a function of decreasing SiO-layer thickness and hence, the resulting decreasing size of the Si-NCs, is demonstrated in Figure 4. The observed PL signal of the crystallized samples can clearly be assigned to quantum-confinement effects.[97] The PL intensity of such a dense array of nearly identical nanocrystals is around two orders of magnitude higher than the PL intensity of a crystallized bulk thick SiO film prepared with the same total thickness. This offers the possibility to use a reduced overall thickness and hence, lower voltages, for device applications. Erbium-doped crystallized samples show a very strong enhancement of the Er^{3+} luminescence by up to three orders of magnitude.[98,99] The energy-transfer process has been shown to be a so-called Förster process and to be very sensitive to the spectral overlap of the Si-NC emission (acting as the "donor") and the absorption states of the Er^{3+} ions (acting as the "acceptor"). Adjusting the crystal size, i.e., the size-dependent bandgap of the Si-NC, to ensure maximum spectral overlap of the two systems results in energy-transfer efficiencies close to 100 %.[99] In this case, the superlattices were produced by SiO evaporation which could be a disadvantage for electrical pumping in terms of a lower breakdown field. Similar superlattices were produced by PECVD, which should show better electrical characteristics.[100] The possibility to control the distance between the individual Si-NCs independently of the nanocrystal size via the stoichiometry x within

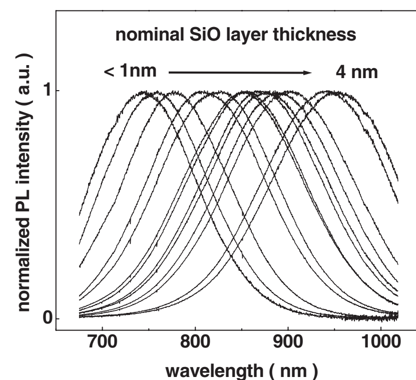

Figure 4. Photoluminescence spectra of a set of SiO/SiO_2 superlattices with layer thicknesses of 1 to 4 nm—i.e., crystals sizes between ~2 and 4 nm. The luminescence was excited by the 325 nm line of an unfocused HeCd laser with a power of 0.17 mW.

the ultrathin SiO_x layers makes this approach very attractive for memory applications.

The last approach mentioned in this section results in a silicon quantum-well structure rather than in Si-NCs. By tightly controlled oxidation of a silicon-on-isolator (SOI) wafer it is possible to create a single layer of ultra-thin single-crystalline Si.[101] The observed PL signal is clearly size dependent and can be explained in terms of quantum-confinement effects. Appropriate lateral structuring of this single crystalline layer in the nanometer range would lead to Si-NCs with defined and equal crystallographic orientations.

3.3. Size-Controlled Si-NC Fabrication from the Gas Phase

The fabrication of Si-NCs from the gas phase is another attractive approach to form a narrow size distribution of nanocrystals. This approach was introduced by Ehbrecht et al.[102] Decomposition of silane in a gas-flow reactor using a CO_2 laser was used to produce crystal sizes between 2 and 20 nm. Time-of-flight mass spectroscopy (TOFMS) shows different velocities for different crystal sizes.[102] A mechanical chopper allows effective size control by velocity selection of the clusters. A schematic of the described setup is shown in Figure 5. The size-controlled Si-NCs can be deposited on any substrate, and patterning of the deposited film is possible.[103] The very good size control was used to show the quantum-confined origin of the strong room-temperature PL signal[104,105] and to analyze different size-dependent effects such as the influence of the size on the photon energies.[102,106] In spite of the very narrow size distribution, the silicon luminescence signal is still quite broad. This unexpected result for these samples was

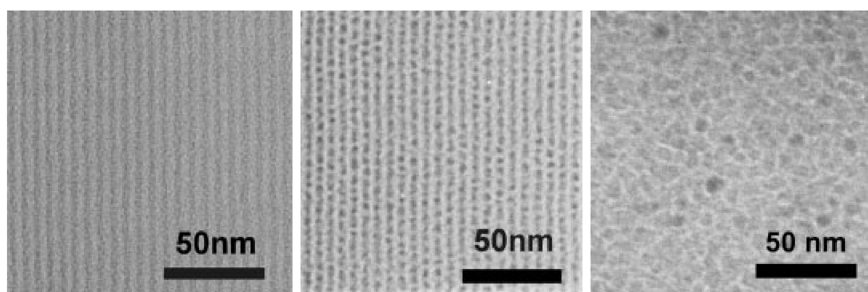

Figure 3. Cross-sectional transmission electron microscopy images of a SiO/SiO_2 superlattice in the amorphous state: a) as-deposited, and b) in the crystallized state after annealing at 1100 °C. The resulting nanocrystals are nearly equal in size and spherical in shape. c) A crystallized SiO bulk layer after annealing at 1100 °C. (Reprinted with permission from [97]. Copyright 2002 Elsevier.)

© 2005 WILEY-VCH Verlag GmbH & Co. KGaA, Weinheim

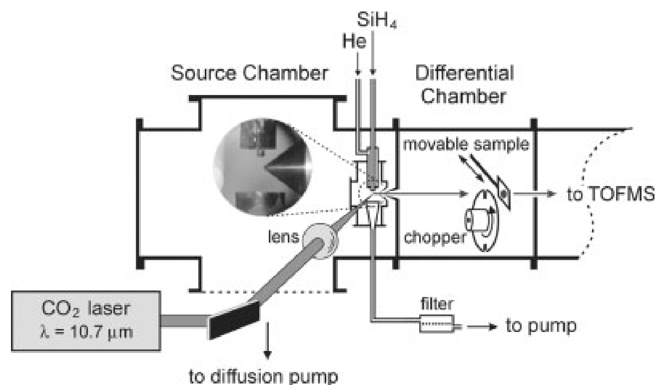

Figure 5. Schematic view of an experimental setup consisting of a cluster beam source and the elements used for deposition. The apparatus contains a laser-driven flow reactor incorporated into the source chamber of a molecular-beam machine and a time-of-flight mass spectrometer. The reactant gas, SiH_4, is admitted to the center of the flow reactor. The gas flow is crossed at right angles with the focused radiation of a pulsed CO_2 laser to initiate the decomposition. The resulting clusters are extracted and analyzed. For more details, see reference [102]. (Figure courtesy of Prof. F. Huisken, Max Planck Institut für Stromungsforschung, Göttingen, Germany.)

explained by size-dependent strain, which introduces an additional broadening due to the different degrees of strain for different crystal sizes.[107] This technique, combined with a projector geometry and the use of suitable masks, can be used to create arbitrarily shaped luminescent structures.[108] The technique and the main results for this class of samples are summarized in a recent overview by Huisken et al.[105]

A similar approach was introduced by Camata et al.[109] Ablation or evaporation of silicon by high-voltage electric-spark discharge was used for silicon-aerosol synthesis. The created aerosols were then ionized by a Kr^{85} β-source and then size-selected by a radial differential-mobility analyzer based on the different charge-to-mass ratios for different crystal sizes. By this method, Si-NCs between 2 and 10 nm were produced. The size control is excellent (standard deviation of less than 10 %). This approach can be adapted to LPCVD or CVD methods. Using conducting-tip AFM, it was possible to store charge in individual Si-NCs deposited on an insulating material by this method.[110]

Orii et al. synthesized silicon aerosols via pulsed-laser ablation of a silicon target in combination with a differential-mobility analyzer.[111] Si-NC sizes between 3 and 6 nm and a size distribution with a FWHM of about 1 nm were produced. In the work of Dutta et al., the synthesis of Si-NCs from the gas phase in SiH_4 plasma growth was shown.[112] The crystal size was about 8 nm. A size-distribution width of about 1 nm was obtained by controlling Ar and H_2 dilution. Single-electron charging effects[113] and tunneling into single nanocrystals were demonstrated on these samples. These experiments benefited from a combination of the specific nanocrystal deposition method and a special contact design.[113] The observed luminescence was attributed to excitons localized at the Si-NC/oxide interface.[114] This assumption was based on the absence of silicon phonon-related structures in the resonantly excited PL signal.

3.4. Single Si-NC Fabrication and Characterization

Besides the need for size control of Si-NCs for potential applications, measurements on single Si-NCs are essential for a better understanding of the optical and electrical phenomena in this material system. Size-controlled Si-NCs grown by the approaches discussed above were used to characterize single Si-NCs within a layer of crystallites by AFM measurements[89,110] or by specifically designed contacts upon which the nanocrystals were deposited.[112] Alternatively, the spatial resolution of a transmission electron microscope was used to measure the conduction band of single Si-NCs by electron energy-loss spectroscopy.[115] Specifically, the methods of creating a single layer of isolated Si-NCs or the deposition of a monolayer of silicon aerosol particles are the preferred candidates for such measurements.

There also exist approaches to synthesize single Si-NCs of a certain size at a given position for electrical or optical characterization. Guo et al.[116] showed the full functionality of a single-electron transistor memory operating at room temperature on a polysilicon dot 9 nm in size. The synthesis of this device was possible due to a combination of electron-beam lithography and reactive-ion etching. The device showed a discrete shift in the threshold voltage, a staircase relation between the charging voltage and the shift, and a self-limiting charging process.

For optical characterization of individual nanocrystals, Valenta et al.[54] used a combination of electron-beam lithography, reactive-ion etching, and subsequent oxidation processes in order to create regular lattices of zero-dimensional silicon nanoparticles, as shown in Figure 6. The luminescence spectra of individual crystals still show a quite broad luminescence signal (FWHM ≈ 120–210 meV) which was attributed to the participation of one or more phonons in the optical transition. In this work, quantum efficiencies of up to 35 % for individual Si-NCs were reported. Similar results were obtained previously[55,117] using a silicon-nanoparticle solution from disintegration of porous silicon and depositing a thin film of the diluted suspension onto a glass coverslip by spin-coating. The spatial resolution of the microscope of the micro-PL setup, 30 µm, allowed detection of the PL signal of individual Si-NCs. The FWHM of the luminescence signal for a single particle was approximately 115 meV. In both cases, the measurements were performed at room temperature. Additional information regarding the recombination process within the Si-NCs could be expected from low-temperature measurements. Such measurements on individual crystals are very unlikely to succeed because of the drastically decreased recombination probability at low temperatures.[4]

 © 2005 WILEY-VCH Verlag GmbH & Co. KGaA, Weinheim

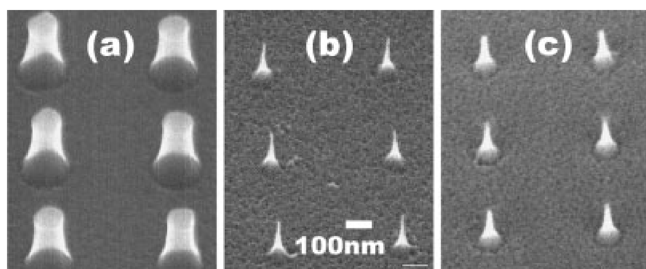

Figure 6. Realization of isolated nanocrystals by using electron-beam lithography and plasma etching to produce a regular matrix of Si pillars, followed by size reduction using a two-stage oxidation. The results are shown in the scanning electron microscopy image of the silicon nanopillars a) after initial patterning, b) following size reduction by thermal oxidation and removal of oxide, and c) following the final oxidation step. (Reprinted with permission from [54]. Copyright 2002 American Institute of Physics.)

4. Conclusions

In this paper, new approaches for controlled Si-NC synthesis by several superlattice approaches, by the synthesis of nanocrystals from the gas phase, and by use of electron-beam lithography were discussed. These techniques allow the synthesis of Si-NCs with diameters between 1 and 20 nm in a size-controlled manner with size distributions with a full width at half maximum of about 1 nm.

A key requirement for most applications is the passivation of the nanocrystal surface, which can be accomplished by several approaches. Well-passivated monodisperse nanocrystals can be produced from the gas phase, as has been shown by the Huisken group,[102,103,105,107] the Atwater group,[109] and by Orii and co-workers.[111] Also possible is the fabrication of superlattices of passivated monodisperse Si-NCs within an SiO_2 matrix by LPCVD and subsequent oxidation,[87] or by the reactive evaporation and phase separation of SiO_x/SiO_2 superlattices.[95] Additionally, in the latter synthesis technique, a high number of periods can be deposited, which facilitates the optical characterization. Due to the narrow size distribution, the quantum-confinement effects and additional migration effects of the excitons could be investigated and separated from each other.[118] The broad FWHM of the luminescence characteristics of ensembles of size-controlled Si-NCs[118] and of individual Si-NCs[54] is assigned to the participation of phonons in the recombination process.

For detailed optical characterization and for applications using Si-NCs as sensitizers for Er^{3+} ions, passivated Si-NCs synthesized via SiO_x/SiO_2 superlattices[95–97] are almost ideally suited. The enormous enhancement of the Er^{3+} luminescence by more than three orders of magnitude due to the adjustment of Si-NC emission and Er^{3+} absorption shows the importance of Si-NC size control and surface passivation for this application.

The synthesis of single passivated layers, either by depositing silicon aerosols onto a substrate or by creating a single layer of passivated Si-NCs by MBE or reactive evaporation of SiO_x, is appropriate for non-volatile memory applications. Recently, Motorola presented a 4 Mbit memory chip based on a single layer of Si-NCs deposited upon a gate oxide.[119] This or similar results could be obtained using any method introduced in this paper, allowing the fabrication of a single layer of isolated Si-NCs.

The various techniques introduced in this paper show great potential for meeting the demands of the suggested applications for this material system. In addition, basic understanding of the luminescence properties and quantum-confinement effects of the indirect semiconductor silicon has been advanced based on the availability of controlled-synthesis techniques for Si-NCs. The key requirements of an independent control of Si-NC size and density, and the importance of surface passivation, can be met by these various synthetic approaches.

Received: July 13, 2004
Final version: December 13, 2004

[1] S. Furukawa, T. Miyasato, *Jpn. J. Appl. Phys., Part 2* **1988**, *27*, L2207.
[2] L. T. Canham, *Appl. Phys. Lett.* **1990**, *57*, 1046.
[3] V. Lehmann, U. Gösele, *Appl. Phys. Lett.* **1991**, *58*, 856.
[4] P. D. J. Calcott, K. J. Nash, L. T. Canham, M. J. Kane, D. Brumhead, *J. Phys.: Condens. Matter* **1993**, *5*, L91.
[5] D. Kovalev, H. Heckler, M. Ben-Chorin, G. Polisski, M. Schwartzkopff, F. Koch, *Phys. Rev. Lett.* **1998**, *81*, 2803.
[6] D. Kovalev, H. Heckler, G. Polisski, F. Koch, *Phys. Status Solidi B* **1999**, *215*, 871.
[7] M. L. Brongersma, P. G. Kik, A. Polman, K. S. Min, H. A. Atwater, *Appl. Phys. Lett.* **2000**, *76*, 351.
[8] G. Franzò, A. Irrera, E. C. Moreira, M. Miritello, F. Iacona, D. Sanfilippo, G. Di Stefano, P. G. Fallica, F. Priolo, *Appl. Phys. A: Mater. Sci. Process.* **2002**, *74*, 1.
[9] C.-X. Du, W.-X. Ni, K. B. Joelsson, F. Duteil, G. V. Hansson, *Opt. Mater. (Amsterdam, Neth.)* **2000**, *14*, 259.
[10] L.-S. Liao, X.-M. Bao, N.-S. Li, X.-Q. Zheng, N.-B. Min, *Solid State Commun.* **1996**, *97*, 1039.
[11] T. Matsuda, M. Nishio, T. Ohzone, H. Hori, *Solid-State Electron.* **1997**, *41*, 887.
[12] M. Wang, X. Huang, J. Xu, W. Li, Z. Liu, K. Chen, *Appl. Phys. Lett.* **1998**, *72*, 722.
[13] H.-Z. Song, X.-M. Bao, N.-S. Li, J.-Y. Zhang, *J. Appl. Phys.* **1997**, *82*, 4028.
[14] C. E. Chryssou, A. J. Kenyon, T. S. Iwayama, C. W. Pitt, D. E. Hole, *Appl. Phys. Lett.* **1999**, *75*, 2011.
[15] G. Franzò, D. Pacifici, V. Vinciguerra, F. Priolo, F. Iacona, *Appl. Phys. Lett.* **2000**, *76*, 2167.
[16] M. Fujii, M. Yoshida, S. Hayashi, K. Yamamoto, *J. Appl. Phys.* **1998**, *84*, 4525.
[17] A. Polman, *J. Appl. Phys.* **1997**, *82*, 1.
[18] P. G. Kik, M. L. Brongersma, A. Polman, *Appl. Phys. Lett.* **2000**, *76*, 2325.
[19] K. Watanabe, M. Fujii, S. Hayashi, *J. Appl. Phys.* **2001**, *90*, 4761.
[20] S. Tiwari, F. Rana, H. Hanafi, A. Hartstein, E. F. Crabbe, K. Chan, *Appl. Phys. Lett.* **1996**, *68*, 1377.
[21] S. Tiwari, F. Rana, K. Chan, L. Shi, H. Hanafi, *Appl. Phys. Lett.* **1996**, *69*, 1232.
[22] A. G. Cullis, L. T. Canham, P. D. J. Calcott, *J. Appl. Phys.* **1997**, *82*, 909.
[23] G. Ghislotti, B. Nielsen, P. Asoka-Kumar, K. G. Lynn, A. Gambhir, L. F. Di Mauro, C. E. Bottani, *J. Appl. Phys.* **1996**, *79*, 8660.
[24] S. Guha, M. D. Pace, D. N. Dunn, I. L. Singer, *Appl. Phys. Lett.* **1997**, *70*, 1207.

 © 2005 WILEY-VCH Verlag GmbH & Co. KGaA, Weinheim

[25] T. Shimizu-Iwayama, N. Kurumado, D. E. Hole, P. D. Townsend, *J. Appl. Phys.* **1998**, *83*, 6018.
[26] T. Shimizu-Iwayama, T. Yoichi, A. Kamiya, M. Takeda, S. Nakao, K. Saitoh, *Nucl. Instrum. Methods Phys. Res., Sect. B* **1996**, *112*, 214.
[27] W. S. Cheong, N. M. Hwang, D. Y. Yoon, *J. Cryst. Growth* **1999**, *204*, 52.
[28] A. J. Kenyon, P. F. Trwoga, C. W. Pitt, G. Rehm, *Appl. Phys. Lett.* **1998**, *73*, 523.
[29] L. He, T. Inokuma, Y. Kurata, S. Hasegawa, *J. Non-Cryst. Solids* **1995**, *185*, 249.
[30] Z.-X. Ma, X.-B. Liao, J. He, W. C. Cheng, G. Z. Yue, Y. Q. Wang, G. L. Kong, *J. Appl. Phys.* **1998**, *83*, 7934.
[31] S. Furukawa, T. Miyasato, *Phys. Rev. B: Condens. Matter Mater. Phys.* **1988**, *38*, 5726.
[32] M. Zacharias, H. Freistedt, F. Stolze, T. Drüsedau, M. Rosenbauer, M. Stutzmann, *J. Non-Cryst. Solids* **1993**, *164–166*, 1089.
[33] M. Zacharias, D. Dimova-Malinovska, M. Stutzmann, *Philos. Mag. B* **1996**, *73*, 799.
[34] H. Seifarth, R. Grötzschel, A. Markwitz, W. Matz, P. Nitzsche, L. Rebohle, *Thin Solid Films* **1998**, *330*, 202.
[35] M. Fujii, A. Mimura, S. Hayashi, D. Kovalev, F. Koch, *Mater. Res. Soc. Symp. Proc.* **2001**, *638*, F9.2.1.
[36] S. Charvet, R. Madelon, R. Rizk, B. Garrido, O. Gonzàlez-Varona, M. López, A. Pérez-Rodríguez, J. R. Morante, *J. Lumin.* **1998**, *80*, 241.
[37] U. Kahler, H. Hofmeister, *Opt. Mater.* **2001**, *17*, 83.
[38] T. Fischer, V. Petrova-Koch, K. Shcheglov, M. S. Brandt, F. Koch, *Thin Solid Films* **1996**, *276*, 100.
[39] S. Chan, P. M. Fauchet, *Appl. Phys. Lett.* **1999**, *75*, 274.
[40] M. L. Brongersma, A. Polman, K. S. Min, E. Boer, T. Tambo, H. A. Atwater, *Appl. Phys. Lett.* **1998**, *72*, 2577.
[41] H. Nishikawa, E. Watanabe, D. Ito, Y. Sakurai, K. Nagasawa, Y. Ohki, *J. Appl. Phys.* **1996**, *80*, 3513.
[42] M. Zhu, Y. Han, R. B. Wehrspohn, C. Godet, R. Etemadi, D. Ballutaud, *J. Appl. Phys.* **1998**, *83*, 5386.
[43] F. Koch, V. Petrova-Koch, *J. Non-Cryst. Solids* **1996**, *198–200*, 840.
[44] Y. Kanemitsu, *Phys. Rev. B: Condens. Matter Mater. Phys.* **1994**, *49*, 16 845.
[45] Y. Kanemitsu, *Phys. Rev. B: Condens. Matter Mater. Phys.* **1996**, *53*, 13 515.
[46] Y. Kanemitsu, S. Okamoto, *Phys. Rev. B: Condens. Matter Mater. Phys.* **1997**, *56*, R15 561.
[47] S. Finkbeiner, J. Weber, M. Rosenbauer, M. Stutzmann, *J. Lumin.* **1993**, *57*, 231.
[48] H. D. Fuchs, M. Stutzmann, M. S. Brandt, M. Rosenbauer, J. Weber, A. Breitschwerdt, P. Deák, M. Cardona, *Phys. Rev. B: Condens. Matter Mater. Phys.* **1993**, *48*, 8172.
[49] M. Stutzmann, M. S. Brandt, M. Rosenbauer, J. Weber, H. D. Fuchs, *Phys. Rev. B: Condens. Matter Mater. Phys.* **1993**, *47*, 4806.
[50] L. Pavesi, *J. Appl. Phys.* **1996**, *80*, 216.
[51] L. Pavesi, M. Ceschini, *Phys. Rev. B: Condens. Matter Mater. Phys.* **1993**, *48*, 17 625.
[52] E. Martin, C. Delerue, G. Allan, M. Lannoo, *Phys. Rev. B: Condens. Matter Mater. Phys.* **1994**, *50*, 18 258.
[53] H. E. Roman, L. Pavesi, *J. Phys.: Condens. Matter* **1996**, *8*, 5161.
[54] J. Valenta, R. Juhasz, J. Linnros, *Appl. Phys. Lett.* **2002**, *80*, 1070.
[55] M. D. Mason, G. M. Credo, K. D. Weston, S. K. Buratto, *Phys. Rev. Lett.* **1998**, *80*, 5405.
[56] ST Microelectronics. http://eu.st.com (accessed October 2002).
[57] Z.-H. Lu, D. J. Lockwood, J.-M. Baribeau, *Nature* **1995**, *378*, 258.
[58] a) D. J. Lockwood, Z. H. Lu, J.-M. Baribeau, *Phys. Rev. Lett.* **1996**, *76*, 539. b) B. T. Sullivan, D. J. Lockwood, H. J. Labbe, Z.-H. Lu, *Appl. Phys. Lett.* **1996**, *69*, 3149.
[59] L. Tsybeskov, K. D. Hirschman, S. P. Duttagupta, M. Zacharias, P. M. Fauchet, J. P. McCaffrey, D. J. Lockwood, *Appl. Phys. Lett.* **1998**, *72*, 43.
[60] C. Ternon, F. Gourbilleau, R. Rizk, C. Dufour, *Physica E (Amsterdam, Neth.)* **2003**, *16*, 517.
[61] L. Tsybeskov, G. F. Grom, M. Jungo, L. Montes, P. M. Fauchet, J. P. McCaffrey, J.-M. Baribeau, G. J. Sproule, D. J. Lockwood, *Mater. Sci. Eng., B* **2000**, *69–70*, 303.
[62] M. Zacharias, J. Bläsing, P. Veit, L. Tsybeskov, K. D. Hirschman, P. M. Fauchet, *Appl. Phys. Lett.* **1999**, *74*, 2614.
[63] M. Zacharias, L. Tsybeskov, K. D. Hirschman, P. M. Fauchet, J. Bläsing, P. Kohlert, P. Veit, *J. Non-Cryst. Solids* **1998**, *227–230*, 1132.
[64] V. Vinciguerra, G. Franzò, F. Priolo, F. Iacona, C. Spinella, *J. Appl. Phys.* **2000**, *87*, 8165.
[65] Z. Ma, L. Wang, K. Chen, W. Li, L. Zhang, Y. Bao, X. Wang, J. Xu, X. Huang, D. Feng, *J. Non-Cryst. Solids* **2002**, *299*, 648.
[66] P. Photopooulos, A. G. Nassiopoulou, D. N. Kouvatsos, A. Travlos, *Mater. Sci. Eng., B* **2000**, *69–70*, 345.
[67] H. J. Trodahl, M. Forbes, D. G. A. Nelson, A. Bittar, *J. Appl. Phys.* **1987**, *62*, 1274.
[68] G. F. Grom, D. J. Lockwood, J. P. McCaffrey, H. J. Labbé, P. M. Fauchet, B. White, J. Diener, D. Kovalev, F. Koch, L. Tsybeskov, *Nature* **2000**, *407*, 358.
[69] T. Tagami, Y. Wakayama, S. I. Tanaka, *Jpn. J. Appl. Phys., Part 2* **1997**, *36*, L734.
[70] M. Zacharias, P. Streitenberger, *Phys. Rev. B: Condens. Matter Mater. Phys.* **2000**, *62*, 8391.
[71] L. Y. Zhu, X. F. Huang, W. B. Fan, X. W. Wang, W. Li, L. Wang, K. J. Chen, *Superlattices Microstruct.* **2002**, *31*, 285.
[72] C. C. Striemer, R. Krishnan, P. M. Fauchet, L. Tsybeskov, Q. Xie, *Nano Lett.* **2001**, *1*, 643.
[73] X. L. Wu, G. G. Siu, S. Tong, Y. Gu, X. N. Liu, X. M. Bao, S. S. Jiang, D. Feng, *Phys. Rev. B: Condens. Matter Mater. Phys.* **1998**, *57*, 9945.
[74] J.-M. Baribeau, D. J. Lockwood, Z. H. Lu, H. J. Labbé, S. J. Rolfe, G. I. Sproule, *J. Lumin.* **1998**, *80*, 417.
[75] R. C. Cammarata, J. C. Bilello, A. L. Greer, K. Sieradzki, S. M. Yalisove, *MRS Bull.* **1999**, *99*, 34.
[76] L. Wang, Z. Ma, X. Huang, Z. Li, J. Li, Y. Bao, J. Xu, W. Li, K. Chen, *Solid State Commun.* **2001**, *117*, 239.
[77] H. Huang, L. Wang, J. Li, W. Li, M. Jiang, J. Xu, K. Chen, *J. Non-Cryst. Solids* **2000**, *266–269*, 1015.
[78] M. Modreanu, M. Gartner, D. Cristea, *Mater. Sci. Eng., C* **2002**, *19*, 225.
[79] F. Bassani, L. Vervoort, I. Mihalcescu, J. C. Vial, F. A. d'Avitaya, *J. Appl. Phys.* **1996**, *79*, 4066.
[80] V. Ioannou-Sougleridis, A. G. Nassiopoulou, T. Ouisse, F. Bassani, F. A. d'Avitaya, *Appl. Phys. Lett.* **2001**, *79*, 2076.
[81] S. Fujita, N. Sugiyama, *Appl. Phys. Lett.* **1999**, *74*, 308.
[82] L. Heikkilä, T. Kuusela, H.-P. Hedman, A. Pavlov, H. Ihantola, *Solid State Phenom.* **1997**, *54*, 13.
[83] G. G. Qin, S. Y. Ma, Z. C. Ma, W. H. Zong, Y. Li-Ping, *Solid State Commun.* **1998**, *106*, 329.
[84] Y. H. Ha, S. Kim, D. W. Moon, J.-H. Jhe, J. H. Shin, *Appl. Phys. Lett.* **2001**, *79*, 287.
[85] M. Zacharias, S. Richter, P. Fischer, M. Schmidt, E. Wendler, *J. Non-Cryst. Solids* **2000**, *266–269*, 608.
[86] J.-H. Jhe, J. H. Shin, K. J. Kim, D. W. Moon, *Appl. Phys. Lett.* **2003**, *82*, 4489.
[87] Y. Hirano, F. Sato, N. Saito, M. Abe, S. Miyazaki, M. Hirose, *J. Non-Cryst. Solids* **2000**, *266–269*, 1004.
[88] T. Baron, F. Martin, P. Mur, C. Wyon, M. Dupuy, *J. Cryst. Growth* **2000**, *209*, 1004.
[89] T. Baron, P. Gentile, N. Magnea, P. Mur, *Appl. Phys. Lett.* **2001**, *79*, 1175.
[90] T. Baron, A. Fernandes, J. F. Damlencourt, B. De Salvo, F. Martin, F. Mazen, S. Haukka, *Appl. Phys. Lett.* **2003**, *82*, 4151.
[91] D. N. Kouvatsos, V. Ioannou-Sougleridis, A. G. Nassiopoulou, *Mater. Sci. Eng., B* **2003**, *101*, 270.
[92] V. Ioannou-Sougleridis, B. Kamenev, D. N. Kouvatsos, A. G. Nassiopoulou, *Mater. Sci. Eng., B* **2003**, *101*, 324.

 © 2005 WILEY-VCH Verlag GmbH & Co. KGaA, Weinheim

[93] T. Müller, K.-H. Heinig, W. Möller, *Appl. Phys. Lett.* **2002**, *81*, 3049.
[94] E. Kapetanakis, P. Normand, D. Tsoukalas, *Appl. Phys. Lett.* **2002**, *80*, 2794.
[95] M. Zacharias, J. Heitmann, R. Scholz, U. Kahler, M. Schmidt, J. Bläsing, *Appl. Phys. Lett.* **2002**. *80*, 661.
[96] L. X. Li, J. Heitmann, M. Schmidt, R. Scholz, U. Kahler, M. Schmidt, J. Bläsing, *Appl. Phys. Lett.* **2002**, *81*, 4248.
[97] J. Heitmann, M. Schmidt, R. Scholz, M. Zacharias, *J. Non-Cryst. Solids* **2002**, *299–302*, 1075.
[98] M. Schmidt, J. Heitmann, R. Scholz, M. Zacharias, *J. Non-Cryst. Solids* **2002**, *299–302*, 678.
[99] J. Heitmann, M. Schmidt, M. Zacharias, V. Y. Timoshenko, M. G. Lisachenko, P. K. Kashkarov, *Mater. Sci. Eng., B* **2003**, *105*, 214.
[100] M. Zacharias, J. Heitmann, L. X. Yi, E. Wildanger, R. Scholz, in *Towards the First Silicon Laser* (Eds: L. Pavesi, S. Gaponenko, L. Dal Negro), NATO Science Series II: Mathematics, Physics, and Chemistry, Vol. 93, Kluwer, Dordrecht, The Netherlands **2003**, p. 131.
[101] Y. Kanemitsu, S. Okamoto, *Phys. Rev. B: Condens. Matter Mater. Phys.* **1997**, *56*, R15 561.
[102] M. Ehbrecht, B. Kohn, F. Huisken, M. A. Laguna, V. Paillard, *Phys. Rev. B: Condens. Matter Mater. Phys.* **1997**, *56*, 6958.
[103] F. Huisken, B. Kohn, V. Paillard, *Appl. Phys. Lett.* **1999**, *74*, 3776.
[104] G. Ledoux, J. Gong, F. Huisken, O. Guillois, C. Reynaud, *Appl. Phys. Lett.* **2002**, *80*, 4834.
[105] F. Huisken, G. Ledoux, O. Guillois, C. Reynaud, *Adv. Mater.* **2002**, *14*, 1861.
[106] V. Paillard, P. Puech, M. A. Laguna, R. Carles, B. Kohn, F. Huisken, *J. Appl. Phys.* **1999**, *86*, 1921.
[107] H. Hofmeister, F. Huisken, B. Kohn, *Eur. Phys. J. D* **1999**, *9*, 137.
[108] G. Ledoux, D. Amans, J. Gong, F. Huisken, F. Cichos, J. Martin, *Mater. Sci. Eng., C* **2002**, *19*, 215.
[109] R. P. Camata, H. A. Atwater, K. J. Vahala, R. C. Flagan, *Appl. Phys. Lett.* **1996**, *68*, 3162.
[110] E. A. Boer, L. D. Bell, M. L. Brongersma, H. A. Atwater, M. L. Ostraat, R. C. Flagan, *Appl. Phys. Lett.* **2001**, *78*, 3133.
[111] T. Orii, M. Hirasawa, T. Seto, *Appl. Phys. Lett.* **2003**, *83*, 3395.
[112] A. Dutta, M. Kimura, Y. Honda, M. Otobe, A. Itoh, S. Oda, *Jpn. J. Appl. Phys., Part 1* **1997**, *36*, 4038.
[113] M. Otobe, H. Yajima, S. Oda, *Appl. Phys. Lett.* **1998**, *72*, 1089.
[114] Y. Kanemitsu, S. Okamoto, M. Otobe, S. Oda, *Phys. Rev. B: Condens. Matter Mater. Phys.* **1997**, *55*, R7375.
[115] P. E. Batson, J. R. Heath, *Phys. Rev. Lett.* **1993**, *71*, 911.
[116] L. Guo, E. Leobandung, S. Y. Chou, *Science* **1997**, *275*, 649.
[117] J. L. Heinrich, C. L. Curtis, G. M. Credo, K. L. Kavanagh, M. J. Sailor, *Science* **1992**, *255*, 66.
[118] J. Heitmann, F. Müller, L. X. Yi, M. Zacharias, D. Kovalev, F. Eichhorn, *Phys. Rev. B: Condens. Matter Mater. Phys.* **2004**, *69*, 195 309.
[119] Motorola. http://www.motorola.com (accessed March 2003).

 © 2005 WILEY-VCH Verlag GmbH & Co. KGaA, Weinheim